Smart Temperature Control With Active Building Occupant Feedback

Santosh K. Gupta * **Koushik Kar** * **Sandipan Mishra** **
John T. Wen *

* *Department of Electrical, Computer, & Systems Engineering (e-mail: guptas7@ rpi.edu, koushik@ecse.rpi.edu, wenj@rpi.edu)*
** *Department of Mechanical, Aerospace and Nuclear Engineering (e-mail: mishrs2@rpi.edu)*
Rensselaer Polytechnic Institute, Troy, NY 12180, USA.

Abstract: In current practice and existing solutions, temperature control in commercial buildings is mostly done independently of occupant feedback. Typically, an acceptable temperature range for the occupancy level is estimated, and the control solution is designed to maintain temperature within that range during occupancy hours while optimizing energy usage at the same time. In this work we incorporate active user (occupant) feedback to minimize aggregate user discomfort. User feedback is accepted in a convenient binary format which is then used to estimate the user's comfort range (discomfort function), taking into account possible inaccuracies in the feedback provided. The control algorithm design also takes the energy cost into account, trading it off optimally with the aggregate user discomfort. A lumped heat transfer model based on thermal resistance and capacitance is used to model a multi-zone building, and singular perturbation theory is utilized to analyze the system. Under sufficient time scale separation between temperature dynamics and user feedback frequency, we establish convergence of the proposed solution to the desired temperature that minimizes the sum of the energy cost plus user discomfort. Simulation results on a four-room example are presented to demonstrate the performance of the proposed approach and validate the model.

Keywords: Temperature control, singular perturbation method, occupant comfort feedback.

1. INTRODUCTION

As a multitude of electronic gadgets make their way into our day-to-day lives, technological innovations are redefining the notion of human comfort, requiring it to be more personalized and adaptive. At the same time, changes in our general living style and expectations are accompanied with a surge in our individual energy demands. This calls for the design of smart systems that can achieve desired human comfort levels without putting additional pressure on energy resources.

Energy usage in buildings, both residential and commercial, account for one major source of energy consumption both within the US and worldwide. Data suggests that nearly 40% of the total energy consumption in US, and 20% of the total energy consumption worldwide, is attributed to the residential and commercial building usage [Lombard et al. (2008)]. More than 75% of current electricity consumption is also due to the usage in buildings. Hence, global energy efficiency cannot be obtained without devising ways for energy efficient operation of buildings. Heating, ventilation, and air conditioning (HVAC) system is one of the major energy consumers in buildings. Numerous design and solution approaches have been proposed for the control and efficiency of HVAC systems. The approaches taken so far can be broadly classified into those focusing on optimal energy usage through variable electricity rates [Sane et al. (2006), Braun (1990), Henze (2005), Henze et al. (2004)], active and passive thermal energy storage [Henze (2005), Henze et al. (2004)], and more recently model predictive control (MPC) approach exploiting information through weather forecast [Ma et al. (2010), Ma et al. (2011), Kelman et al. (2011), Ma and Borrelli (2012), Gatsis and Giannakis (2011)].

Any commercial building combined with its occupants is a complex network of heterogeneous and inter-connected subsystems. The major objective of an HVAC system is attaining occupant comfort. Energy conservation or energy efficiency goals require integrating (or trading off) this objective with minimum energy consumption. The building and its occupants combined are thus a single entity for which the HVAC control needs to be optimized. However, most of the existing approaches treat the building and its occupants as separate entities, and a typical building temperature control system is designed independent of the occupant feedback. An acceptable temperature range for the given (or perceived) occupancy level is estimated and the control system aims to maintain the temperature within that range. This is a fragmented approach towards attaining energy efficiency in buildings, and in general will be sub-optimal. A smart building energy control system that seeks and takes into account the comfort level feedback of its occupants to determine the HVAC control input is likely to be more efficient. This can however be a challenging task in large commercial buildings such as schools, libraries, offices etc. which have a very diverse collection of occupants. A diverse group of occupants will have different ranges of comfort as well as different tolerance levels towards temperature variations beyond their individual comfort ranges. Since the location of the occupants in a building is not static, and even their comfort preferences could change over time, a temperature control system that is based on a-priori knowledge of occupant location and preferred temperature range is not desirable. In other words, the system needs to learn these dynamically through user (occupant) feedback and incorporate it into the control strategy. Therefore, achieving energy efficiency in a building taking into account the comfort levels of its occupants needs a new and unique approach towards problem solution.

In this paper we present a control solution to optimally tradeoff the overall energy cost with the aggregate occupant discomfort. A novel algorithm is developed and analyzed using gradient optimization and singular perturbation theory. We use simple feedback from users in the form of 'heat up' or 'cool down', which are further consolidated to estimate their comfort ranges or the discomfort functions, taking into account possible errors in the users' feedback close to the boundaries of their comfort range. The user input thus obtained when combined with the resulting energy cost, determines the direction in which the energy control input is adjusted. We consider a multi-zone building, and use a lumped heat transfer model based on thermal resistance and capacitance for system analysis. Singular perturbation theory is used to analyze the system, with temperature evolution on a faster time scale and user input on a relatively slower time scale. With this time scale separation, the proposed control algorithm achieves convergence to a desired temperature that minimizes the sum of total energy cost and the aggregate user discomfort. Simulation results are presented for a four-room model to demonstrate the performance and effectiveness of the proposed algorithm. It is worth noting that our work is loosely related to Thermovote [Erickson and Cerpa (2012)] and a more recent work [Purdon et al. (2013)] that seek user feedback at binary/multiple levels, and determine the direction of temperature adjustment based on the average user vote. However, unlike these existing studies, we pose the problem formally as an optimization question that takes into account the temperature dynamics as a function of the energy input. Furthermore, while we prove that our control solution converges to the optimal tradeoff point between energy cost and user discomfort, no such guarantees are known to hold for the existing approaches.

2. SYSTEM MODEL AND CONTROL ALGORITHM

We first present a model for the building infrastructure and obtain the equations governing the system, and then pose the temperature control problem as a convex optimization question. We then describe a control law whose stability and optimality is established in Section 3.

2.1 Problem Formulation

The first major step towards designing a building energy control system is determining the choice of the building heat transfer model. Different models towards this purpose have been proposed in the literature, which include the finite element method based model [Mebee (2011)], lumped mass and energy transfer model [Riederer et al. (2002), Wu et al. (2008)], and graph theoretic model based on electrical circuit analogy [Boyer et al. (1996), Fraisse et al. (2002), Xu et al. (2008), Athienitis et al. (1985)]. The system model selection entails a tradeoff between computational efficiency and accuracy of representation of the temperature dynamics. The electrical analogy approach to modeling multiple interconnected zones reduces the heat transfer model to an equivalent electrical circuit network. The model can be further modified to include building occupancy, room and heating equipment dynamics [Athienitis et al. (1985), Chandan (2010)]. In this paper we take this electrical circuit analogy approach, and combine it with occupant discomfort feedback modeling.

A building is modeled as a collection of interconnected zones, with energy/temperature dynamics evolving according to a lumped heat transfer model. In the lumped heat transfer model, a single zone is modeled as a thermal capacitor and a wall is modeled as an RC network. This results in the standard lumped 3R2C wall model [Fraisse et al. (2002)]. The heat flow modeling is based on temperature difference and thermal resistance: $Q = \Delta T/R$, where ΔT is the temperature difference, R is the thermal resistance and Q is the heat transferred across the resistance. This is analogous to the current due to voltage difference across a resistor. Also, note that the thermal capacitance denotes the ability of a space to store heat: $C\frac{\mathrm{d}\Delta T}{\mathrm{d}t} = Q$.

The heat flow and thermal capacitance model can be written for all the thermal capacitors in the system, with T_i as the temperature of the ith capacitor. Consider the system to have n thermal capacitors and l thermal resistors. With additional sources of heat input such as ambient environment, we can write the overall heat transfer model of the system with m zones as [Mukherjee et al. (2012)]:

$$C\dot{T} = -DR^{-1}D^T T + B_0 T_\infty + Bu + Bw, \qquad (1)$$

where $T \in \mathbb{R}^n$ is the temperature vector (representing the temperature of the thermal capacitors in the 3R2C model), $u \in \mathbb{R}^m$ is the vector of heat inputs into the different zones of the building, and $B \in \mathbb{R}^{n\times m}$ is the corresponding input matrix. Also, note that (T, u) are functions of time $(T(t), u(t))$ and accordingly $\dot{T} = \frac{dT}{dt}$. Note that positive values of u correspond to heating the system while negative values of u correspond to cooling. In the above equation, $C \in \mathbb{R}^{n\times n}$ consists of the wall capacitances and is a diagonal positive definite matrix; $R \in \mathbb{R}^{l\times l}$ consists of the thermal resistors in the system and is a diagonal positive definite matrix as well. Also, $D \in \mathbb{R}^{n\times l}$ is the incidence matrix, mapping the system capacitances to the resistors, and is of full row rank [Lombard et al. (2008)], and $B_0 = -DR^{-1}d_0^T \in \mathbb{R}^n$ is a column vector with non-zero elements denoting the thermal conductances of nodes connected to the ambient. Further, T_∞ is the ambient temperature, and $w \in \mathbb{R}^m$ is the thermal noise in the different zones. We represent the snapshot of the above parameters in Table 1 below for quick reference.

In this study we neglect the thermal noise, and so our model equation (1) becomes:

$$C\dot{T} = -DR^{-1}D^T T + B_0 T_\infty + Bu. \qquad (2)$$

In our model, the zones are picked such that each of them has a heating/cooling unit, which in turn implies that B is of full row rank. Also, since matrix D is of full row rank the product $DR^{-1}D^T$ is a positive definite matrix. The vector of zone temperatures, denoted by y (which is a function of T) can be expressed as,

$$y = B^T T. \tag{3}$$

Our overall minimization objective (overall cost) is the sum of two terms: (i) energy cost (i.e., cost of heating/cooling), and (ii) aggregate discomfort cost of the occupants. The energy cost (i) is expressed as $\frac{1}{2}u^T \Gamma u$, where Γ is a positive definite matrix. Note that the energy cost is quadratic in the heat input vector u [Mukherjee et al. (2012)], and is consistent with other works such as [Kelman et al. (2011)] which approximates energy cost as a quadratic function of the mass flow rate. Furthermore, our framework and analysis also extends to other convex energy costs. Let S_j denote the set of all occupants in zone j, and $\rho = \sum_{j=1}^{m} |S_j|$ be the total number of occupants in the building. Also let G_s denote the (convex) discomfort function of occupant s in zone j. Then the aggregate occupant discomfort cost (ii) is expressed as $\sum_{j=1}^{m}\sum_{s\in S_j} G_s(y_j(T))$, where $y_j(T) = [B^T T]_j$ from (3) denotes the j^{th} element of y, or the temperature of zone j. Our minimization objective is thus expressed as,

$$U(u,T) = \frac{1}{2}u^T \Gamma u + \gamma \sum_{j=1}^{m}\sum_{s\in S_j} G_s(y_j(T)). \tag{4}$$

In (4), γ is a scalar constant that defines the relative weight provided to the aggregate occupant discomfort, as compared to the energy cost. Next we obtain a control strategy that can guide the control input u so that it minimizes the total system cost as defined in (4) subject to the temperature dynamics (2) and (3).

2.2 Solution Approach

Assuming a constant ambient temperature T_∞, and using equilibrium condition (setting $\dot{T} = 0$ in (2)) we obtain:

$$T = h(u) = (DR^{-1}D^T)^{-1}(B_0 T_\infty + Bu). \tag{5}$$

$$\text{Define, } J(u) = U(u, h(u)), \tag{6}$$

i.e., $J(u)$ is obtained by plugging in $T = h(u)$ from (5) into (4). Note that energy cost term in (4) is strictly convex in u; and the aggregate occupant term is convex in T, and therefore convex in u when T is set to $h(u)$, since $h(u)$ is affine in u. This implies that $J(u)$ is strictly convex in u. Therefore $J(u)$ has a unique optimal solution u^*. Define

$$T^* = h(u^*), \tag{7}$$

Table 1. Snapshot of the system parameters.

Parameter	Definition
$T \in \mathbb{R}^n$	Temperature vector
$u \in \mathbb{R}^m$	Heat input vector
$C \in \mathbb{R}^{n\times n}$	Wall capacitances
$R \in \mathbb{R}^{l\times l}$	Thermal resistors in the system
$D \in \mathbb{R}^{n\times l}$	Incidence matrix
$B_0 \in \mathbb{R}^n$	Thermal conductances of nodes connected to the ambient
$T_\infty \in \mathbb{R}^n$	Ambient temperature
$w \in \mathbb{R}^m$	Thermal noise
$B \in \mathbb{R}^{n\times m}$	Input matrix

which is also unique by definition.

With the goal of driving the system to (u^*, T^*), we propose the control input u be updated once every Δ time units as

$$u_{k+1} = u_k - \eta\big(\Gamma u + \gamma Y \Lambda F(y)\big), \tag{8}$$

where η is a scalar that can be loosely interpreted as the "feedback gain" of the system. Furthermore, $Y \in \mathbb{R}^{m\times m}$ in the above is the Jacobian obtained using (3) and the equilibrium condition (5), expressed as

$$Y = (\frac{\partial y}{\partial u}) = B^T(DR^{-1}D^T)^{-1}B. \tag{9}$$

Also, $\Lambda \in \mathbb{R}^{m\times\rho}$ is the zone-occupant matrix that indicates which occupants are present in a zone ($\Lambda_{js} = 1$ if $s \in S_j$, and 0 otherwise), and $F(y) \in \mathbb{R}^{\rho\times 1}$ is the "marginal discomfort" vector of the occupants, obtained by taking partial derivative of the occupant discomfort functions with respect to y. In other words, the s^{th} element of $F(y)$, where $s \in S_j$, is obtained as

$$F_s(y_j) = \frac{\mathrm{d}G_s(y_j)}{\mathrm{d}y_j}, \quad s \in S_j. \tag{10}$$

Comparing (8) with (4) provides the motivation of our control algorithm: roughly speaking, (8) updates u in the gradient direction of $U(u,T)$, while taking in account the relationship between T and u at equilibrium, as given by (5). In other words, it attempts to update u is the direction of $-\nabla J(u)$, where $J(u)$ is defined by (6). In this interpretation, η represents the constant "step size" associated with the gradient descent.

Note however that using (4) - (6), $\nabla J(u)$ is expressed as:

$$\nabla J(u) = \Gamma u + \gamma Y \Lambda F(B^T h(u)). \tag{11}$$

From (11) we note that update of u in the gradient direction of $J(u)$ requires user discomfort feedback at $y = B^T h(u)$, the equilibriated zone temperatures corresponding to u. In practice, however, a user $s \in S_j$ will provide a comfort feedback at the current temperature it experiences, $y_j = [B^T T]_j$ (different in general from the equilibriated temperature $[B^T h(u)]_j$), which is what we incorporate into our control algorithm as stated in (8). This implies that our control algorithm as described in (8) does not exactly move u in the gradient direction ($-\nabla J(u)$). The effect of this difference (error) can be analyzed using *singular perturbation theory* [Khalil (2002), Kokotovic et al. (1986)], which in our case requires (for convergence to optimality) that the occupant feedback be collected after long intervals (i.e. Δ is large), allowing the temperature T to settle down close to $h(u)$ before the next occupant feedback collection.

Towards developing a singular perturbation model of our system, we first consider a continuous approximation to the evolution of the control input u:

$$\dot{u} \approx \frac{u_{k+1} - u_k}{\Delta} = -\frac{\eta}{\Delta}\big(\Gamma u + \gamma Y \Lambda F(y)\big). \tag{12}$$

Note that time step Δ is the interval at which user feedback is solicited and the control input u is updated. A larger Δ implies a slower evolution of u. We next express the system evolution in the time scale of the evolution of u (slower time scale as compared to the time scale at which T evolves). Define $\epsilon = \frac{1}{\Delta}$ as the perturbation parameter; then $\tau = \frac{t}{\Delta} = \epsilon t$ is the slower time scale. Then

$$\frac{\mathrm{d}\tau}{\mathrm{d}t} = \epsilon \implies \dot{u} = \frac{\mathrm{d}u}{\mathrm{d}t} = \epsilon\Big(\frac{\mathrm{d}u}{\mathrm{d}\tau}\Big); \quad \dot{T} = \frac{\mathrm{d}T}{\mathrm{d}t} = \epsilon\Big(\frac{\mathrm{d}T}{\mathrm{d}\tau}\Big). \quad (13)$$

Control input equation (12) can now be expressed in terms of τ as follows, using the fact that $y = B^T T$:

$$\frac{\mathrm{d}u}{\mathrm{d}\tau} = -\eta\big(\Gamma u + \gamma Y \Lambda F(B^T T)\big). \quad (14)$$

Similarly, equation (2) modeling the temperature evolution of the building can now be expressed as:

$$C\epsilon\frac{\mathrm{d}T}{\mathrm{d}\tau} = -DR^{-1}D^T T + B_0 T_\infty + Bu. \quad (15)$$

Equations (14) and (15) represent a singularly perturbed system. Note, $\Delta \uparrow \implies \epsilon \downarrow$ leading to steady state condition for temperature evolution. In the next section as we establish the global asymptotic stability of our system as given by equations (14) and (15).

Finally, note that implementation of our control algorithm would require that $F_s(y_j)$, the "marginal discomfort" value of user s in zone j at the current zonal temperature $y_j = [B^T T]_j$, be reasonably estimated from the discomfort feedback of s at any time. In practice, the occupants may provide the feedback in some simple form describing their actual level of discomfort ("I am feeling hot", "I am feeling very cold" etc.). This feedback must be processed to estimate the marginal discomfort (derivative of the actual discomfort function), as we do in our simulation study described in Section 4.

3. STABILITY ANALYSIS

The system evolution is governed by the set of equations (14) and (15). In equation (15) the coefficient $DR^{-1}D^T$ is positive definite which makes the unforced system (with $u = 0$) exponentially stable. We use singular perturbation analysis [Kokotovic et al. (1986)] to establish the condition for stability of the system.

Next we introduce Lyapunov functions $V(u)$ and $W(u, T)$ that will be used in our stability analysis:

$$V(u) = J(u) - J(u^*), \text{ and} \quad (16)$$

$$W(u, T) = (T - h(u))^T P (T - h(u)), \quad (17)$$

where P in the above equation is a symmetric positive definite matrix (the exact choice of matrix P will be determined at a later stage). We now define a combined Lyapunov function $L(u, T)$:

$$L(u, T) = (1 - \alpha)V(u) + \alpha W(u, T), \quad (18)$$

where α satisfies $0 < \alpha < 1$.

We start by evaluating the conditions to establish stability using Theorem 2.1 and Corollary 2.1 from chapter 7 of [Kokotovic et al. (1986)]. We propose the following comparison functions for the analysis:

$$\Psi(u) = \|\nabla J(u)\|, \text{ and} \quad (19)$$

$$\Phi(T - h(u)) = \|T - h(u)\|. \quad (20)$$

We assume that the user discomfort function $G_s(y_j)$ has bounded second derivative i.e. there exists a $\tilde{\kappa} < \infty$:

$$\frac{\mathrm{d}^2 G_s(y_j)}{\mathrm{d}^2 y_j} \le \tilde{\kappa}, \forall y_j, s \in S_j. \quad (21)$$

Note that from equation (10) above:

$$F_s^{'}(y_j) = \frac{\mathrm{d}F_s(y_j)}{\mathrm{d}y_j} = \frac{\mathrm{d}^2 G_s(y_j)}{\mathrm{d}^2 y_j} \le \tilde{\kappa}, s \in S_j. \quad (22)$$

We can now use the Mean Value Theorem to assert:

$$F_s(y_j) - F_s\big([B^T h(u)]_j\big) = F_s^{'}(\tilde{y}_j)\big(y_j - [B^T h(u)]_j\big),$$
$$\text{for some } \tilde{y}_j \in (y_j, [B^T h(u)]_j), s \in S_j. \quad (23)$$

Applying Cauchy-Schwartz inequality on (23), for $s \in S_j$:

$$\|F_s(y_j) - F_s\big([B^T h(u)]_j\big)\| \le \|F_s^{'}(\tilde{y})\| \|y_j - [B^T h(u)]_j\|. \quad (24)$$

Define $\kappa = \tilde{\kappa}\|B^T\|$. Then from (24), (22) and (3), we have

$$\|F(y) - F(B^T h(u))\| \le \kappa \|(T - h(u))\|. \quad (25)$$

Now we evaluate the conditions in Assumption 2.3 [chapter 7 of Kokotovic et al. (1986)] on $V(u)$ to obtain:

$$\frac{\partial V}{\partial u}\Big(\frac{\mathrm{d}u}{\mathrm{d}\tau}\Big|_{h(u)}\Big) = -\eta(\nabla J(u))^T(\nabla J(u)) \le -\eta\Psi^2(u), \quad (26)$$

$$\text{and} \quad \frac{\partial V}{\partial u}\Big(\frac{\mathrm{d}u}{\mathrm{d}\tau}\Big|_T - \frac{\mathrm{d}u}{\mathrm{d}\tau}\Big|_{h(u)}\Big)$$
$$= -\eta\gamma(\nabla J(u))^T Y \Lambda\big(F(y) - F(B^T h(u)\big)$$
$$\le \eta\gamma\kappa\|Y\|\|\Lambda\|\Psi(u)\Phi(T - h(u)). \quad (27)$$

The above expressions are obtained by taking partial derivative of $V(u)$ as defined in (16) and substituting $\frac{\mathrm{d}u}{\mathrm{d}\tau}$ from (14). Next, evaluating conditions from Assumption 2.2 [chapter 7 of Kokotovic et al. (1986)] on $W(u, T)$ yields (28) and (29), stated below.

$$\frac{\partial W}{\partial T}\Big(\epsilon\frac{\mathrm{d}T}{\mathrm{d}\tau}\Big) = -2(T - h(u))^T P C^{-1}(DR^{-1}D^T)(T - h(u))$$
$$\le \quad -2\lambda_{min}\Phi^2(T - h(u)), \quad (28)$$

where λ_{min} is the minimum eigenvalue of the symmetric part of the matrix $(PC^{-1}DR^{-1}D^T)$, assumed to be positive definite. Note that the symmetric positive definite matrix P must be chosen such that $(PC^{-1}DR^{-1}D^T)$ is positive definite. One choice would be $P = C$ since $(DR^{-1}D^T)$ is positive definite. Another choice is $P = I$; it is reasonable to assume that the symmetric part of the matrix $(C^{-1}DR^{-1}D^T)$ has positive eigenvalues, as we have verified to hold for the data set used in our simulation study presented in the next section.

$$\frac{\partial W}{\partial u}\Big(\frac{\mathrm{d}u}{\mathrm{d}\tau}\Big|_T\Big) = 2\eta(T - h(u))^T P(DR^{-1}D^T)^{-1}B\nabla J(u)$$
$$+ 2\eta\gamma(T - h(u))^T P(DR^{-1}D^T)^{-1}BY\Lambda\big(F(B^T T) - F(B^T h(u)\big)$$
$$\le 2\eta\|P\|\|(DR^{-1}D^T)^{-1}\|\|B\|\Psi(u)\Phi(T - h(u))$$
$$+ 2\eta\gamma\kappa\|P\|\|(DR^{-1}D^T)^{-1}\|\|B\|\|Y\|\|\Lambda\|\Phi^2(T - h(u)). \quad (29)$$

Equation (28) is obtained using (15) and the definition of $W(u, T)$ in (17). Equation (29) is obtained using (17) as well as (14), (11) and (25). Given the Lyapunov functions $V(u)$ and $W(u, T)$ satisfy the conditions (26) - (29) and are radially unbounded by definition, Theorem 2.1 with Corollary 2.1 of [Kokotovic et al. (1986)] states that for every α, $L(u, T)$ as given by equation (18), is a Lyapunov function for $\epsilon < \epsilon^*$. For our system ϵ^* can be obtained in terms of the conditions derived in equations (26) - (29):

$$\epsilon^* = \frac{\lambda_{min}}{2\eta\gamma\kappa\|P\|\|(DR^{-1}D^T)^{-1}\|\|B\|\|Y\|\|\Lambda\|}. \quad (30)$$

Note that $L(u, T)$ is minimized uniquely at (T^*, u^*). It follows therefore that (T^*, u^*) is a globally asymptotically stable equilibrium point for all $\epsilon < \epsilon^*$, or all $\Delta > \Delta^*$.

4. SIMULATION

In this section we present simulation results of our proposed control algorithm. For the simulations we consider a four-room building from an example in [Moore et al. (2011)], which is illustrated in Figure 1 below. Heat transfer to the ambient for all rooms is added to the model. In the figure, each double headed arrow represents a ther-

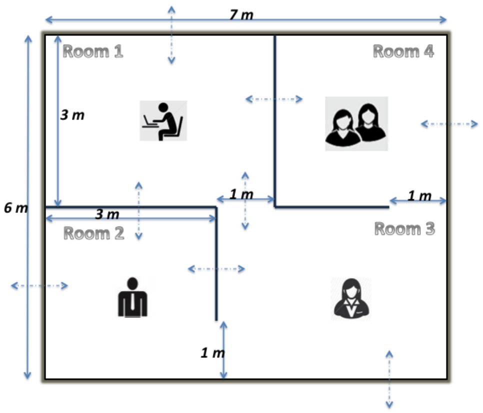

Fig. 1. Four room example model used for simulation. Each room has occupancy as illustrated in the figure.

mal connection between the two corresponding sides. The connection between two rooms through an open door is represented by a single resistance, and the same through the wall is represented using 3R2C wall model. The simulation results presented in this work have been obtained with two users (occupants) in room 4, and one user each in the other three rooms.

For this example model of four rooms and eight walls, we get 20 capacitive elements and 27 resistive elements. This gives us the dimensions of the incidence matrix, D for the model as 20 $\times$ 27. Using the dimensions of the model in Figure 1, volumetric heat capacity values and thermal resistance values as per [Mukherjee et al. (2012)], we can obtain values for the matrices in equation (2). Using this information we simulate the model with ambient temperature at $T_\infty = 15°C$. The building temperature is allowed to fall to the ambient when it is unoccupied. In this study we have picked the occupant feedback interval Δ as five minutes. We present results for the general scenario when the users in different zones have different comfortable temperature ranges. The system was observed to converge to the desired (optimal) temperature for each zone.

We first present the basic results in Figures 3 and 4 to show convergence. The system starts with a default common temperature range that is comfortable for all occupants as depicted in first row of Table 2. The subsequent rows of the same table indicate the real comfortable temperature range for each occupant. Note that these values are not explicitly indicated by the user, but conveyed implicitly to the system through user feedbacks. In our simulation we assume that a user is required to submit feedback in a simple binary form, indicating whether he/she is feeling hot or cold in the current setting. The lack of feedback from the user is assumed to be an indication that the user is currently comfortable. Based on the received user feedback the system constantly estimates the comfortable range (discomfort function) for each user and controls the temperature accordingly.

We recognize the fact that user feedback around the boundaries of its comfortable temperature range can be somewhat imprecise. This is taken into account in our simulation by associating a probability distribution with the user feedback in a δ range around the comfort range boundaries. More precisely, if y_s^U is the upper limit of the comfort range of user s in zone j, the feedback of the user changes from 0 (no feedback, or the user feels comfortable) to 1 (user feels hot) linearly as y_j varies in the range $[y_s^U - \delta, y_s^U + \delta]$. A similar probability distribution is also associated for user feedback in the range $[y_s^L - \delta, y_s^L + \delta]$, where y_s^L is the lower limit of the user's comfort range. For this simulation study we have used the value of δ as 1. Note that this practical consideration would also account for slight changes in the upper and lower limit of comfortable temperature with the user's mood and attire. This is depicted in Figure 2 below. Also, in our simulation we assume a convex user discomfort function of the form:

$$G_s(y_j) = \begin{cases} 2(y_j - y_s^U)^2 & \text{if } y_j > y_s^U, \\ 0 & \text{if } y_s^L \leq y_j \leq y_s^U, \\ 2(y_j - y_s^L)^2 & \text{if } y_j < y_s^L, \end{cases} \tag{31}$$

where y_s^U and y_s^L are the upper and lower limit temperatures, respectively, of the user s located in zone j.

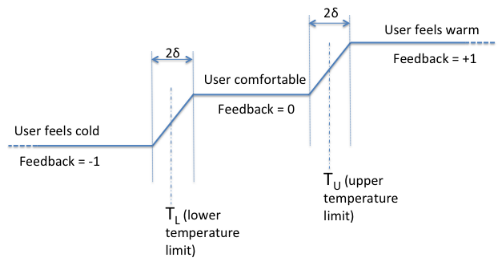

Fig. 2. Linear probability distribution applied to user feedback at the lower and upper temperature limits. δ denotes the range around the limit values in which probabilistic distribution is applied.

The results presented in Figures 3 and 4 are for a simulation run over a 5 hour period, when all the users get in at 7am and stay for a 5 hour period before breaking off for lunch hour. The results show that the temperature and control (heat) input converges. The converged temperatures were verified to minimize the weighted sum of the energy usage and aggregate user discomfort, subject to allowed lower and upper constraints on the temperature.

Table 2. Each user's range of comfortable temperature. Users 4 and 5 occupying room 4 have a common range of temperature comfort.

	Low Temp. (° C)	High Temp. (° C)
Range (all users)	17	27
Range (U1)	21	23
Range (U2)	19	22
Range (U3)	20	22
Range (U4)	21	24
Range (U5)	20	23

The evolution and convergence of the simulated system is dependent on the values of three major model parameters,

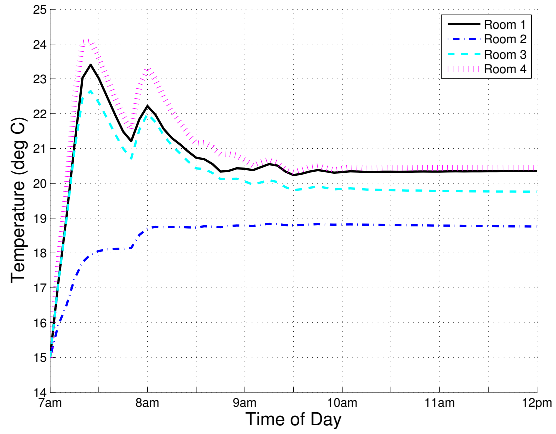

Fig. 3. Temperature evolution of the 4 room model over a 5 hour period with the rooms occupied throughout the period as per Figure 1. The user temperature preference is as per Table 2.

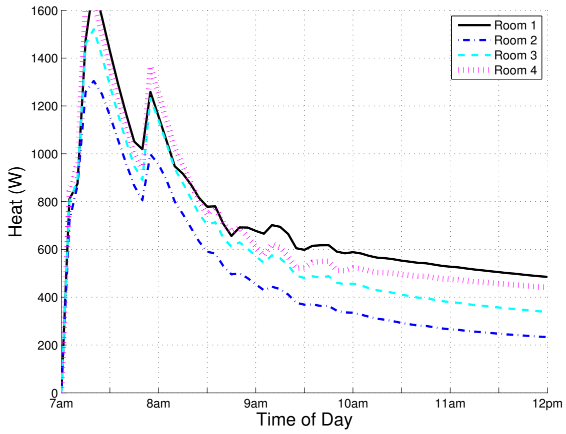

Fig. 4. Heat (control) input for the 5 hour period simulation with uninterrupted occupancy, and user temperature preference as in Table 2.

feedback gain (step size) parameter (η), user feedback weight parameter (γ), and heat cost parameter (Γ). The feedback gain (step size) parameter controls the size of change in u in each step. Small values of η would lead to a very slow convergence of the system to the desired temperature. With a high value of η we can hit the desired range of temperature much faster, but at the cost of high temperature overshoots resulting in much higher total heat input. Also, a sufficiently high value of η could violate the time scale separation assumption that is needed for stability. In our study, η was tuned to obtain a reasonable trade-off. Another important parameter of the model, user weight parameter (γ), signifies the weight given to the penalty associated with the building occupant discomfort. A higher γ would result in a high value of control input for a given user comfort feedback vector. This in turn would cause the temperature to change sharply as a result of user discomfort, but may also result in large overshoots as well as higher energy costs. In our simulations, γ was tuned to obtain a reasonable trade-off between energy cost and user discomfort level. In this study we use a time varying heat cost factor Γ. Once the last user leaves the building we increase the value of Γ, so that heat input (energy) is minimized during non-occupant hours.

Table 3. 48 hour period user schedule for the model from figure 1. U1+ marks the entry of user occupying room 1 and U1− indicates user leaving the corresponding room.

	7 am	8 am	9 am	12 to 1 pm	4 pm	5 pm	6 pm
Day 1	(Sim Start) U1+	U2+	U3, U4, U5+	Lunch Hour	U1−	U2−	U3, U4, U5−
Day 2		U3, U4, U5+	U1, U2+	Lunch Hour		U3, U4, U5−	U1, U2−
Day 3	(Sim End)						

4.1 Multi-user, common temperature preference

The scenarios simulated in Figures 3 and 4, where the users all arrive at the same time, and stay in their respective rooms for several hours, do not represent a typical real world scenario. We next present simulation results on the model over a 48 hour period in a typical office environment. The building occupants move in and out as per the schedule shown in Table 3. Room 4 is occupied by two users U4 and U5. We consider two different cases for the users of room 4. First case corresponds to both the users of room 4 having a common range of comfortable temperature range as shown in Table 2. The temperature and control input over the 48 hour period is shown in Figures 5 and 6. In Figure 7 we show the corresponding user feedback input per room, obtained as the derivative of their discomfort function (level of discomfort that they express), as in (10). The simulation starts at 7am when the first user occupying zone 1 gets into office. The zone is at its initial temperature of $15°C$. The user provides the feedback that it is cold which results in additional heat input to the building. One hour later (at 8 am) user occupying zone 2 gets in, and all other users come in at 9 am. The temperature quickly converges to the desired comfortable range and stays there until the users step out for lunch hour at 12 pm. At this point the heat input is reduced in the building and the temperature starts falling towards the ambient to conserve energy. Once the users get back in from lunch (at 1 pm) and provide feedback the heat is adjusted to quickly drive the temperature to comfortable range again. The heat input starts dropping again, as users start leaving starting 4 pm. At the end of day when the last user steps out (at 6 pm), heat input to the building is almost immediately reduced, and the temperature keeps falling overnight. Next day, users arrive in different order: zone 3 and 4 users at 8am, and zone 1 and 2 users at 9am. All of them step out for lunch hour at 12pm. Finally the users step out at the end of day: zone 3 and 4 users at 5pm and zone 1 and 2 users at 6pm. The temperature follows the user occupancy pattern to optimize energy usage.

Figure 7 shows the user feedback history over the 48 hour period of model simulation. A positive (negative) value of feedback corresponds to the user feeling warm (cold) in the current temperature. Positive (negative) user feedback would result in cooling (heating) of the room in the next

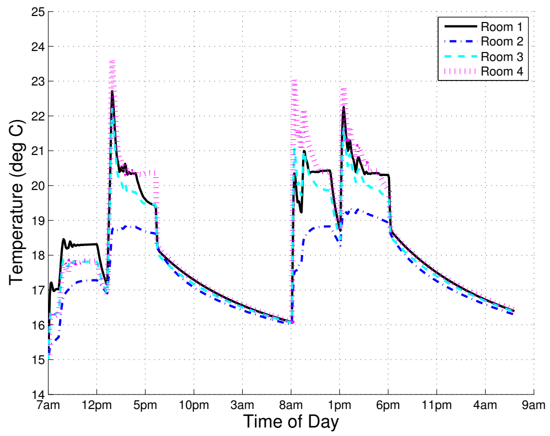

Fig. 5. Temperature profile of the model from Figure 1 over a 48 hour period. User schedule follows Table 3 and temperature preferences Table 2.

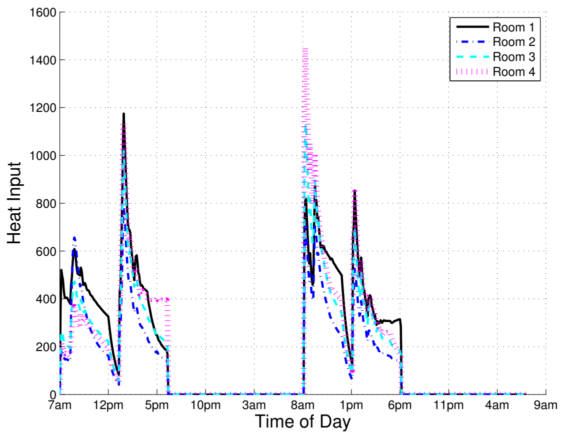

Fig. 6. Heat input over a 48 hour period simulation. User schedule from Table 3 and temperature preferences per Table 2.

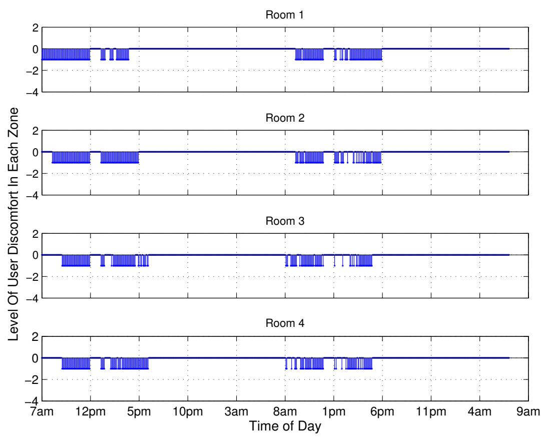

Fig. 7. User feedback per zone depicting their comfort level with the current temperature they experience.

update cycle. Note that for room 4 which has two users U4 and U5, the input determines the overall direction that the control needs to take in that room.

4.2 Multi-user conflicting temperature preference

The second case corresponds to the users 4 and 5 (occupying room 4), having a conflicting temperature preference. The consolidated temperature range of all the users is shown in Table 4. The temperature evolution with the corresponding heat input in Figures 8 and 9. In this scenario since there is no common comfortable range for both the users of room 4, its not possible to satisfy both the users simultaneously. Hence, the temperature of room 4 settles between 23°C and 24°C, which minimizes the total discomfort level for the two users given their conflicting preferences. The overall heat consumed is higher when compared to the earlier case.

Table 4. Each user's range of comfortable temperature. Users 4 and 5 occupying room 4 now have conflicting temperature preferences.

	Low Temp. (° C)	High Temp. (° C)
Range (all users)	17	27
Range (U1)	21	23
Range (U2)	19	22
Range (U3)	20	22
Range (U4)	21	23
Range (U5)	24	25

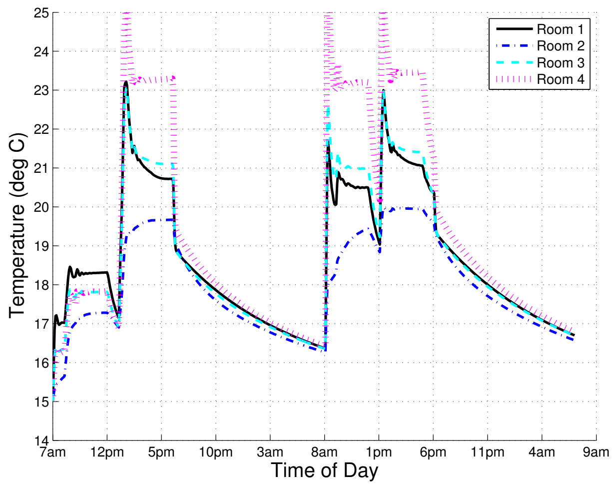

Fig. 8. Temperature profile of the Figure 1 model for 48 hour period. User schedule per Table 3 and temperature preference per Table 4.

5. CONCLUSION AND FUTURE WORK

In this paper, we demonstrate that the building temperature and energy usage can be controlled successfully and efficiently through dynamic feedback from the users (occupants) based on their comfort levels. Under the reasonable assumption that user feedback is provided at a slower time scale as compared to the building temperature dynamics, our analysis shows that the proposed control algorithm results in the desired (optimal) trade-off between energy usage and user discomfort. The simulation study presented further shows that with effective tuning of a few parameters, the control algorithm attains a fast temperature convergence rate with reasonable energy expenditure. The binary form of the feedback that we have experimented

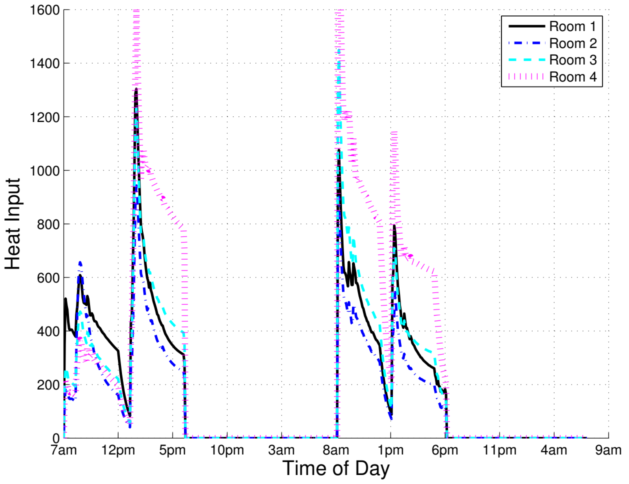

Fig. 9. Heat input over a 48 hour period simulation with user schedule following Table 3 and temperature preference as shown in Table 4.

with in our simulations provide a convenient way for users to indicate their preferences to the control system.

While we have relied on the RC model of a building to develop and analyze our optimal control solution, it is worth noting that the control law described in (8) is reasonably 'model independent' which is a very desirable goal from a practical implementation standpoint. The term in (8) that depends on the building model is the Jacobian matrix Y which is given by (9). While we have assumed knowledge of Y in our simulations, in practice the matrix of resistances R could be estimated through measurements or calculations using the building's structural parameters. Y can thus be estimated from (9). In practice the matrix Y would be sparse owing to low coupling between zones far apart in a building. Effective estimation or approximation of Y, and performance effects of estimation inaccuracies, will be investigated in future work.

REFERENCES

Athienitis, A., Chandrashekhar, M., and Sullivan, H. (1985). Modelling and analysis of thermal networks through subnetworks for multizone passive solar buildings. *Applied Mathematical Modelling*, 9.

Boyer, H., Chabriat, J., Grondin-Perez, B., Tourrand, C., and Brau, J. (1996). Thermal building simulation and computer generation of nodal models. *Building and Environment*, 31.

Braun, J. (1990). Reducing energy costs and peak electrical demand through optimal control of building thermal storage. *ASHRAE transactions.*

Chandan, V. (2010). Modelling and control of hydronic building hvac systems. *Master's thesis, University of Illinois at Urbana Champaign.*

Erickson, V.L. and Cerpa, A.E. (2012). Thermovote: participatory sensing for efficient building hvac conditioning. *BuildSys '12 Proceedings of the Fourth ACM Workshop on Embedded Sensing Systems for Energy-Efficiency in Buildings*, Toronto, ON, Canada.

Fraisse, G., Viardot, C., Lafabrie, O., and Achard, G. (2002). Development of simplified and accurate building model based on electrical analogy. *Energy and Buildings*, 34, 1017–1031.

Gatsis, N. and Giannakis, G. (2011). Residential demand response with interruptible tasks: Duality and algorithms. *In Proceedings of 50th IEEE Conference on Decision and Control and European Control Conference.*

Henze, G. (2005). Energy and cost minimal control of active and passive building thermal storage inventory. *Journal of Solar Energy Engineering*, 127.

Henze, G., Felsmann, C., and Knabe, G. (2004). Evaluation of optimal control for active and passive building thermal storage. *International Journal of Thermal Sciences*, 40.

Kelman, A., Ma, Y., and Borrelli, F. (2011). Analysis of local optima in predictive control for energy efficient buildings. *In Proceedings of 50th IEEE Conference on Decision and Control and European Control Conference.*

Khalil, H. (2002). *Nonlinear Systems (Chp. 11)*. Prentice-Hall, 3rd edition.

Kokotovic, P., Khalil, H., and O'Reilly, J. (1986). *Singular Perturbation Methods in Control: Analysis and Design.* London: Academic Press.

Lombard, L., Ortiz, J., and Pout, C. (2008). A review on buildings energy consumption information. *Energy and Buildings*, 40, 394–398.

Ma, Y., Anderson, G., and Borrelli, F. (2011). A distributed predictive control approach to building temperature regulation. *In Proceedings of American Control Conference.*

Ma, Y. and Borrelli, F. (2012). Fast stochastic predictive control for building temperature regulation. *In Proceedings of American Control Conference*, Montreal, Canada.

Ma, Y., Borrelli, F., Hencey, B., Coffey, B., Bengea, S., Packard, A., Wetter, M., and Haves, P. (2010). Model predictive control for the operation of building cooling systems. *In Proceedings of American Control Conference.*

Mebee, B. (2011). Computational approaches to improving room heating and cooling for energy efficiency in buildings. *PhD thesis, Virginia State and Polytechnic Institute.*

Moore, K., Vincent, T., Lashlab, F., and Liu, C. (2011). Dynamic consensus networks with application to the analysis of building thermal processes. *In Proceedings of 18th IFAC World Congress*, Milane, Italy.

Mukherjee, S., Mishra, S., and Wen, J. (2012). Building temperature control: A passivity-based approach. *IEEE 51st Annual Conference on Decision and Control.*

Purdon, S., Kusy, B., Jurdak, R., and Challen, G. (2013). Model-free hvac control using occupant feedback. *IEEE 38th Conference on Local Computer Networks Workshops (LCN Workshops)*, Sydney, NSW.

Riederer, P., Marchio, D., Visier, J., Husaunndee, A., and Lahrech, R. (2002). Room thermal modelling adapted to the test of hvac control systems. *Building and Environment*, 37.

Sane, H., Haugstetter, C., and Bortoff, S. (2006). Building hvac control systems - role of controls and optimization. *Proceedings of American Control Conference.*

Wu, Z., Stoustrup, J., and Heiselberg, P. (2008). Parameter estimation of dynamic multi-zone models for livestock indoor climate control. *In Proceedings of 29th*

AIVC Conference on advanced building ventilation and environmental technology for addressing climate change issues.

Xu, B., Fu, L., and Di, H. (2008). Dynamic simulation of space heating systems with radiators controlled by trvs in buildings. *Energy and Buildings*, 40.